PERFORMANCE ANALYSIS OF DEEP LEARNING TECHNIQUES IN AIRCRAFTS CLASSIFICATION

UMUT ÇİMEN

SEPTEMBER 2024

ÇANKAYA UNIVERSITY

GRADUATE SCHOOL OF NATURAL AND APPLIED SCIENCES

DEPARTMENT OF ELECTRICAL AND ELECTRONICS ENGINEERING

M.Sc. Thesis in

ELECTRICAL AND ELECTRONICS ENGINEERING

PERFORMANCE ANALYSIS OF DEEP LEARNING TECHNIQUES IN AIRCRAFTS CLASSIFICATION

UMUT ÇİMEN

SEPTEMBER 2024

ABSTRACT

PERFORMANCE ANALYSIS OF DEEP LEARNING TECHNIQUES IN AIRCRAFTS CLASSIFICATION

ÇİMEN, UMUT

M.Sc. in Electrical and Electronics Engineering

Supervisor: Assoc. Prof. Dr. Barbaros PREVEZE

September 2024, 51 Pages

With the developing technologies in recent years, many attack and defense systems are needed. The most prominent area of this need is the aviation sector. Many aircraft operate national or international flights during the day. However, there may be possible attacks. Detection of aircraft is of great importance in order to prevent this situation and take the necessary precautions. In this study, it is aimed to analyze the performance of deep learning techniques on aircraft classification.

In this study, GoogleNet and ResNet18 are used in image classification techniques. Random test and learning classes with different percentages are created for approximately 5000 aircraft images in the ready-made dataset, which includes 5 separate classes: Passenger Aircraft, Military Aircraft, Helicopter, Drone and Rocket. According to the results of these test and learning classes, it is decided to continue with 90% learning and 10% test classes, as a generally higher performance rate is observed in the results with more training data. While the data input size of ResNet18 and GoogleNet architectures are 224x224x3, the data inputs are changed and training is performed 5 times with 90% training class of 210x210x3, 230x230x3 and 250x250x3 dimensions and the average values of the results are taken. These values have shown us that; better performances can be achieved by changing the data sizes, compared to the results given by the original methods. With Googlenet 210x210x3 data entry, a better percentage of performance has been achieved for criticality situations.

It has been observed that with RestNet18 230x230x3 data entry, an acceptable level of lower performance was achieved in case of time criticality, but less than half of the time was saved.

Keywords: Deep Learning Techniques, Aircraft Classification, Googlenet, ResNet18, Image Classification, Aircraft Detection

ÖZET

HAVA ARAÇLARININ SINIFLANDIRILMASINDA DERİN ÖĞRENME TEKNİKLERİNİN PERFORMANS ANALİZİ

ÇİMEN, UMUT
Elektronik ve Haberleşme Mühendisliği Yüksek Lisans

Danışman: Doç. Dr. Barbaros PREVEZE
Eylül 2024, 51 Sayfa

Son yıllarda gelişen teknolojilerle birlikte çok sayıda saldırı ve savunma sistemlerine ihtiyaç duyulmaktadır. Bu ihtiyacın en önde gelen alanı da havacılık sektörüdür. Bir çok hava aracı gün içerisinde ulusal veya uluslar arası uçuşlar gerçekleştirmektedir. Bununla birlikte olası saldırı ihtimalleri olabilecektir. Bu durumunu önüne geçmek ve gerekli tedbirleri alabilmek için hava araçlarının tespiti büyük önem taşımaktadır. Bu çalışmada derin öğrenme tekniklerinin hava aracı sınıflandırılması üzerindeki performans analizi amaçlanmıştır.

Bu çalışmada görüntü sınıflandırma tekniklerinde GoogleNet ve ResNet18 kullanılmıştır. Yolcu uçağı, Askeri uçak, Helikopter, Drone ve Roket olmak üzere 5 ayrı sınıf içeren hazır datasette bulunan yaklaşık 5000 hava aracı görüntüsü için farklı yüzdelerde rastgele test ve öğrenme sınıfları oluşturulmuştur. Bu test ve öğrenme sınıflarından çıkan sonuçlara göre eğitim verisinin fazla olduğu sonuçlarda genel olarak daha yüksek başarım oranı gözlendiği için %90 öğrenme ve %10 test sınıfları ile devam edileceği kararlaştırılmıştır. ResNet18 ve GoogleNet mimarilerinin veri giriş boyutu 224x224x3 iken, veri girişleri değiştirilerek 210x210x3, 230x230x3 ve 250x250x3 boyutlarında %90 eğitim sınıfı ile 5'er kere eğitim yapılmıştır ve sonuçların ortalama değerleri alınmıştır. Bu değerler de bize göstermektedir ki; veri boyutlarının değiştirilmesi ile orijinal yöntemlerin vermiş olduğu sonuçlara göre daha iyi performanslar elde edilebilmiştir. Googlenet 210x210x3 veri girişi ile başarım oranı kritikliği durumları için daha iyi bir yüzde elde edilmiştir. RestNet18 230x230x3 veri girişi ile zaman kritikliği durumunda ise kabul edilebilir düzeyde daha düşük başarım ancak yarı yarıyadan daha kısa bir süre tasarrufu sağlandığı gözlenmiştir.

Anahtar Kelimeler: Derin Öğrenme Teknikleri, Uçak Sınıflandırma, Googlenet, ResNet18, Görüntü Sınıflandırma, Uçak Tespiti

ACKNOWLEDGEMENT

I would like to express my deepest gratitude to my esteemed thesis advisor, Assoc. Prof. Dr. Barbaros Preveze, for his unwavering support and guidance throughout this project. His profound knowledge and mentorship have been invaluable in completing this thesis. Additionally, I am profoundly grateful to my family, especially my parents, for their constant belief in me and their unwavering support both financially and emotionally. To my dear sister, I extend special thanks for her continuous encouragement and assistance. Finally, to my beloved spouse, who has stood by me with patience and love, I am endlessly thankful for your support and understanding throughout this challenging journey. It is thanks to all of you that I have reached this point, and it is an honor to celebrate this achievement with you.

TABLE OF CONTENTS

LIST OF TABLES

LIST OF FIGURES

LIST OF ABBREVIATIONS

CNN	: Convolutional Neural Network
EEG	: Electroencephalography
FN	: False Negative
FP	: False Positive
TN	: True Negative
TP	: True Positive
TUSP	: Thyroid Ultrasound Standard Plane
UAV	: Unmanned Aerial Vehicle
YOLO	: You-Only-Look-Once

CHAPTER I
INTRODUCTION

With the developing technology in health, military, agriculture, and many other fields, much data, such as images and signals, are collected. To increase the efficiency of the studies in these fields, it is important that the collected data can be processed automatically. This automation can have advantages such as reducing manpower and saving time. Due to the rapid developments in scientific and technological fields, accurate and sensitive image detection and classification have become important for high-efficiency analysis [1]. The classification of the mentioned data is also one of the data processing methods. It is seen that CNNs are used in this field for classification. When the literature is examined, in a study conducted in the health field [2], a real-time detection approach based on an EEG signal was adopted to detect epileptic seizures. In the samples taken from a total of 22 patients (5 males and 17 females), a 97.74% accuracy rate was obtained using GoogleNet. This example can be shown as an example of signal processing methods.

As an example of image classification, a study was conducted to classify Thyroid Ultrasound Standard Plane (TUSP) images, which are the basis for automatic diagnosis of thyroid diseases in the health field, with high accuracy. In this study, where the ResNet18 model was used, 83.88% accuracy was obtained [3]. Many image classification studies have been conducted in other areas and with different methods in the health field [4-6].

In the research conducted by Tien-Heng Hsieh and Jean-Fu Kiang, 1D-CNN and 2D-CNNs were selected for the classification of agricultural land images and achieved 99.8% and 98.1% success rates, respectively [7]. Leila Hashemi-Beni and Asmamaw Gebrehiwot performed image classification for crop-weed discrimination in agricultural fields. In the study, where U-Net and FCN-8 convolutional neural network models were used, there are 60 images of an organic carrot field. In weed detection, FCN-8 performed better with a 75.1% success rate than U-Net which achieved a 66.72% success rate. However, in crop detection, the U-net model

performed better with a 60.48% success rate compared to FCN-8, which achieved a 47.86% success rate [8].

The main purpose of this study is the classification of aircrafts. When classifying aircrafts, the aim should be to achieve the highest possible classification performance. In the priority of Security and Defense, precise identification and categorization of aircraft is vital in military operations to identify enemy aircraft and protect friendly aircraft. Incorrect categorization can cause significant security vulnerabilities. The most important factors are taking the necessary precautions against military aircraft, distinguishing passenger aircraft and ensuring passenger safety [9]. When looking at similar examples in the literature, it is seen that different studies have been done with different data sets. In the study conducted by Hao Liu and his colleagues in 2018 [10], they integrated the system established with HD cameras with image classification in order to eliminate the deficiency in the detection of small drones. Yolo V2 was used to classify the dataset containing 30000 data. By creating random training and test classes, 52.13% success was achieved for Drone, 90.47% for Helicopter, and 96.03% for Aircraft. J Chen and his friends have worked on the classification of aircraft types. Due to the lack of publicly available datasets, they used a ready-made dataset and this dataset contains 3594 images. In this study, using the T-SEN algorithm, a 70% success rate was achieved [11]. Sarah Bolton and his friends presented a backup structure in order to prevent possible errors or losses due to the sharing of aircraft estimates made by Automatic Dependent Surveillance-Broadcast (ADS-B) in text form and performed image classification for aircraft. A dataset of 10000 images covering 100 different models was used. Each image was rearranged according to model, manufacturer, or variant information. An average of 98.5% success rate was achieved by using CMAL-Net as an image processing model [12]. Yangeng Wang et al. proposed the hybrid BA-CNN structure, which is an aircraft recognition algorithm, due to the difficulty of detecting various aircraft types and their similarities. The depth of this network was increased by using the two-channel ResNet34 structure. In this study, 89.2% success was achieved using 10000 aircraft data [13]. In another study, friend-foe classification in aircraft was done using the classical artificial neural network method, and 99.93% success was achieved [14].

This study aims to classify multi-class aircraft, and since this classification can affect important areas such as country borders and air defense security in military terms, high performance is targeted. When the literature is examined, there are not

many studies for this purpose. Various situations have been addressed in previous studies in this field. The first of these is class diversity in aircraft classification. Numerous studies in the literature focus on categorizing aircraft using various Convolutional Neural Network (CNN) architectures. Typically, these studies focus only on civil aircraft or certain types of military aircraft and it has been observed that they use a limited category range with certain datasets. Another issue is dataset diversity. Most of the studies in the literature are focused on civil aircraft such as commercial aircraft and helicopters. There is a lack of research covering a wider class range such as military aircraft, rockets and unmanned aerial vehicles. In particular, there is no study on the dataset used in this study. In this study, a comprehensive dataset consisting of military jet aircraft, passenger aircraft, helicopters, drones and missiles was used. Therefore, a more comprehensive categorization system was created. The aim of this study is to evaluate the performance of common CNN models, such as ResNet-18 and GoogleNet on aircraft classification and provide important findings regarding model selection in the industry. It is also aimed that this study will contribute to the literature and the military field.

CHAPTER II
ABOUT DATASET

Aircraft are machines that are aimed to operate with the zero-error principle and are used in many areas such as transportation, reconnaissance, military operations, transportation, and rescue. In this study, a dataset prepared by Abdul Waheed, which is available on Kaggle and divided into five separate classes, will be considered [15]. The images in this dataset were taken from a Google image search. The classes in the dataset are military jet aircraft, helicopters, passenger aircraft, unmanned aerial vehicles (UAVs), and rockets. Passenger aircraft are aircraft developed to transport hundreds of passengers from one point to another in the safest way, thanks to their long structures. Although helicopters are slow in speed with their vertical take-off and landing capabilities, they have more advantages regarding the area they can reach. Military aircraft are distinguished from other aircraft by their much faster and more flexible structures thanks to their reinforced jet engines and aerodynamics. Drones can be controlled remotely or operate autonomously and are small and light aircraft that are generally used in reconnaissance, surveillance, and mapping missions. Rockets play an important role in obtaining meteorological data, both in attacks and satellite launches, thanks to their powerful engines that can start from a short diameter and extend beyond the atmosphere.

2.1 MILITARY JET AIRCRAFT

Armed forces use Military aircraft for purposes such as hitting targets in wars, destroying other aircraft, conducting reconnaissance, and carrying ammunition [16].

Fighter aircraft are designed to destroy enemy elements using the ammunition integrated into them [17]. They differ from other aircraft due to their sharp lines, powerful engines, and the ammunition they carry. The Military Jet Aircraft image in the dataset used in this study is shown in Figure 1.

Figure 1: Military Jet Aircraft [15]

2.2 HELICOPTER

Helicopters are rotary-wing aircraft capable of vertical takeoff and landing. They are used especially in areas such as rescue operations, military missions, logistic support, and short-distance passenger transportation. Flexible and maneuverable helicopters can provide transportation even in difficult terrain conditions. The helicopter has a horizontally rotating helicopter rotor system that provides lift and thrust. This allows the helicopter to take off and land vertically (VTOL), hover in the air, and fly forward, backward, and laterally [18]. This rotary-wing structure is the most important feature distinguishing helicopters from other aircraft. The Helicopter image in the dataset used in this study is shown in Figure 2.

Figure 2: Helicopter [15]

2.3 PASSENGER AIRCRAFT

Passenger planes are aircraft manufactured solely to carry passengers. They can carry many passengers with their long and wide body structure. In addition to passengers, they are also used to transport passengers' luggage and partly other materials. Passenger planes are generally known as high-capacity and high-performance aircrafts by airline companies commercially. In addition to these, light aircraft that carry fewer passengers and are generally used for short distances have similar structures. Passenger planes are frequently preferred transportation vehicles, especially for inter-country trips, due to their time-saving nature. The Passenger Aircraft image in the dataset used in this study is shown in Figure 3.

Figure 3: Passenger Aircraft [15]

2.4 DRONE

Unmanned aerial vehicles (UAVs) or drones [19] are aircraft that do not physically have humans inside. The most important component of drones is a communication system between a ground-based controller and the aircraft [20]. UAVs are divided into two classes: those that are controlled by a remote controller and those that can move automatically on a predetermined flight path. Although they were initially produced for reconnaissance purposes, they have been developed over time and are now used in attack missions. In addition, UAVs have recently been used for purposes such as firefighting and agricultural irrigation. The Drone image in the dataset used in this study is shown in Figure 4.

Figure 4: Drone [15]

2.5 MISSILE

A missile is a self-propelled, air-propelled ranged weapon, typically powered by a propellant, jet engine, or rocket engine. It is designed for various military applications, including strategic defense, precision strikes, and air defense operations. Missiles can be equipped with different types of warheads depending on their intended use, from explosive charges to specialized munitions aimed at specific targets. The Missile image in the dataset used in this study is shown in Figure 5.

Figure 5: Missile [15]

The dataset utilized in this study contains 1867 Military Jet, 1387 Helicopter, 1424 Passenger aircraft, 1332 Drone and 1334 Missile images. However, these numbers were reduced because some data were not suitable for our study. The distribution of images in each class is shown in Table 1.

Table 1: Distribution of the Dataset [15]

Image Types	Military Jet Aircraft	Helicopter	Passenger Plane	Drone	Missile
Number of Images	1429	1074	868	1223	980

CHAPTER III
IMAGE CLASSIFICATION

Image classification is the task of assigning a label or class to an entire image. Images are expected to have only one class per image. Image classification models take an image as input and return a prediction of which class the image belongs to. The goal of the classification process is to categorize all pixels in a digital image into one of several land cover classes or “themes.” This categorized data can then be used to produce thematic maps of the land cover found in an image. Normally, multispectral data is used to perform the classification, and in fact, the spectral pattern found in the data for each pixel is used as the numerical basis for the classification. The goal of image classification is to identify and depict the features occurring in an image as a unique gray level (or color) in terms of the object or land cover type.

Image classification generally consists of Data Collection and Preparation, Image Feature Extraction, Model Training, Model Testing and Evaluation, and Categorization sections.

The data collection and preparation phase come first for the classification process. It is essential to collect the necessary photographs and label these images. Labeling provides information about the class to which each image belongs. The dataset is used to train the model.

It is necessary to extract certain features from the photographs. This can be defined as specifying important features such as color tone, consistency and boundaries. This process, which was previously performed manually, is now done using deep learning methodologies. Thus, errors such as calculation and oversight can be prevented.

After the creation of the features, the image classification model is trained using these created features. Deep learning techniques, especially convolutional neural networks (CNNs), are extremely effective in this procedure. The model completes training on image classes using training data.

After the training phase, the model's accuracy is evaluated using test data. In this step, the model's performance is evaluated using real data. Accuracy, precision, recall, and F1 score are generally used as success criteria.

Once the model is trained and evaluated, it can be used to categorize new, unlabeled photographs. Based on the results, predictive algorithms are used to determine the classification of a particular image.

3.1 DEEP LEARNING AND CONVOLUTIONAL NEURAL NETWORKS

Convolutional neural networks (CNNs) have significantly transformed the domain of picture classification. These networks have specialized layers that can detect specific characteristics inside images and convert these characteristics into more complex and abstract representations [21]. Figure 6 basically shows the CNN structure.

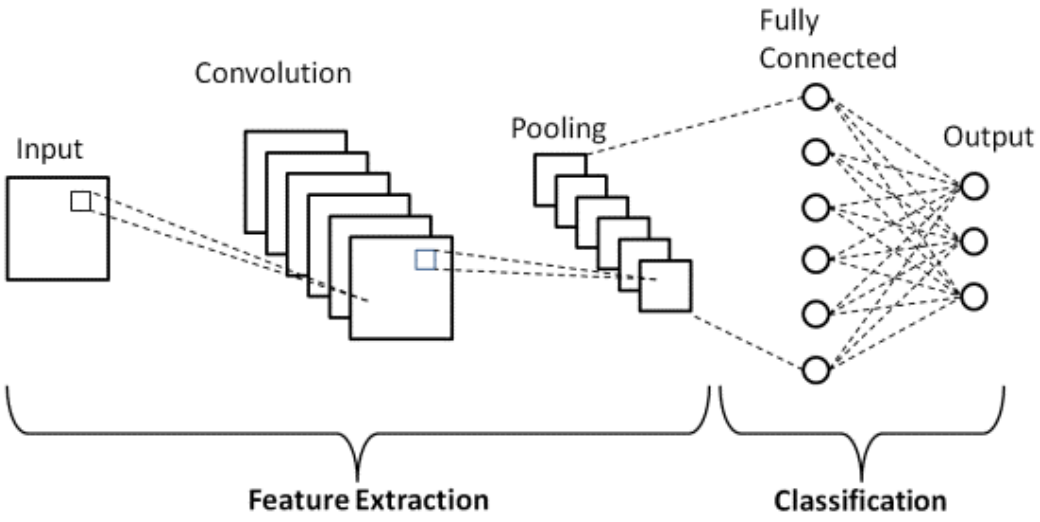

Figure 6: The Structure of CNN [22]

The main CNN layers used in deep learning are convolutional layers, pooling layers, and fully connected layers.

- **Convolutional Layers:** Convolutional neural networks are used to create a feature map from the image as input data for classification. The aim is to determine a guide for the image whose feature is created and calculate the convolution between this guide and each part of the input image. Thus, when the input color is an image, a three-dimensional pixel matrix representing the height, width, and depth, which are the RGB equivalents of the image, is created [23]. The calculation of the convolution layer is shown in equation 3.1.

$$C_i = f\left(\sum_{j=1}^{n}(W_i * X_j) + b_j\right) \quad (3.1)$$

where f is the activation function, W_i represents the convolutional kernels for the ith output feature map, X_j represents the j th input feature map, and b_j is the bias term for the i th output feature map [24].

- **Pooling Layers:** Pooling layers are also known as down-sampling layers. Pooling layers are the basic components of Convolutional Neural Networks (CNNs) that perform dimensionality reduction. The number of parameters in the input is reduced and the computational load is significantly reduced. This process increases the efficiency of the model. There are two basic types of pooling: max pooling and average pooling [25].

  In Max Pooling, as the filter moves along the input, the pixel with the maximum value in the receptive field is selected and this value is sent to the output array. Max pooling is widely used because it can capture the significant features in the input data. The calculation of the max pooling is shown in equation 3.2.

$$S_i = \underset{i \in R_j}{max} h_i \quad (3.2)$$

where *h* is some pixel in the subregion *Rj* in the feature map [26].

In Average Pooling, as the filter moves along the input, the average value of the pixels in the receptive field is calculated and this average value is sent to the output array. The calculation of the average pooling is shown in equation 3.3.

$$S_j = \frac{1}{n}\sum_{i \in R_j}^{n} h_i \quad (3.3)$$

where *h* is some pixel in the subregion *Rj* in the feature map and *n* is the number of features in the subregion where subsampling is required [26].

Figure 7 shows the pooling process, max pooling, and average pooling.

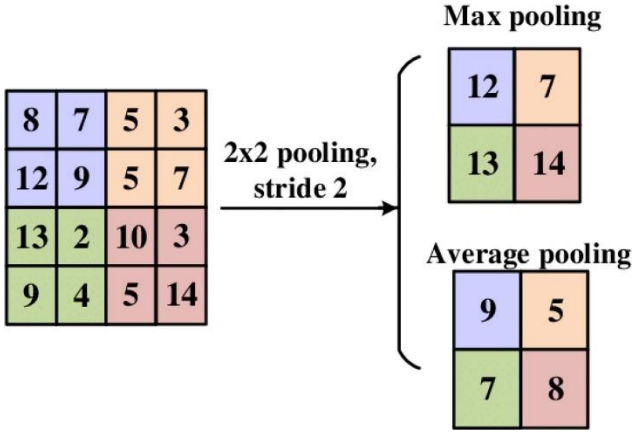

Figure 7: Pooling Layers [24]

- **Fully Connected Layers:** The final step of Convolutional Neural Networks occurs in this layer. Fully Connected Layers are an artificial neural network in which all nodes and neurons in a layer of the architecture are connected to the next layers. This type of network is computationally complex and prone to overload. After the Flattening process is applied to the obtained data, the learning process with neural networks is applied. Simply put, in this layer, the matrix data that passes through the Convolutional Layer and Pooling Layers many times is turned into a flat vector [27]. The calculation of the fully connected layer is shown in equation 3.4.

$$y = f(Wx + b) \tag{3.4}$$

Where; y is the output vector of the layer, W is the weight matrix of shape, x is the input vector of shape, b is the bias vector of shape

Figure 8 shows the fully connected layer model.

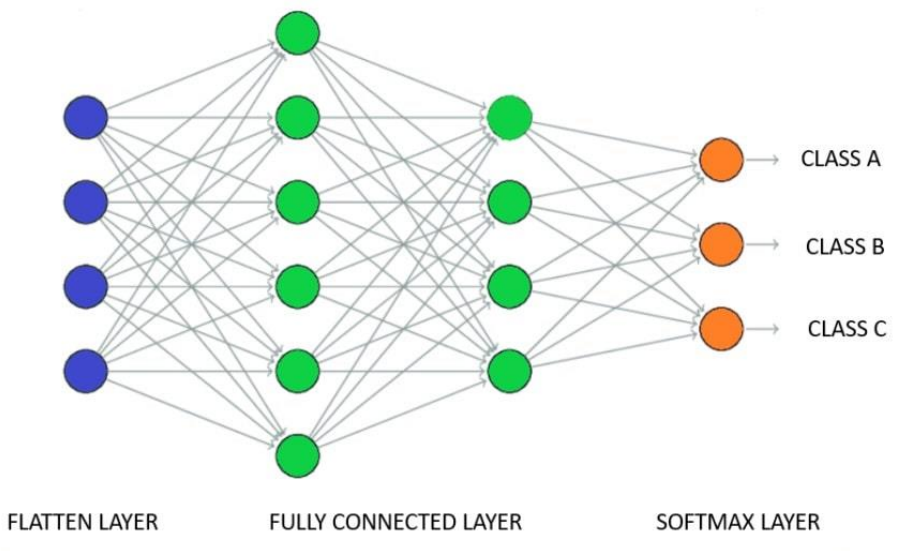

Figure 8: Fully Connected Layers [24]

3.2 EVALUATION METRICS

In this study, two different models were used to classify aircraft. To evaluate the classification performance of both models, accuracy, precision, recall, and confusion matrix were mainly used to measure the effectiveness of the models. For multiple classifications, we divide the samples into four samples based on their true categories and categories predicted by machine learning: True Positive (TP), False Positive (FP), True Negative (TN), and False Negative (FN). When TP, FP, TN and FN represent the corresponding number of samples, TP +FP +TN +FN represents the total number of samples [28].

The percentage of samples that the classifier successfully identified compared to all of the samples is known as accuracy which is calculated as shown in equation 3.5;

$$Accuracy = \frac{TP + TN}{TP + TN + FP + FN} \tag{3.5}$$

Precision is the percentage of examples labeled as positive that are positive which is calculated as shown in equation 3.6;

$$Precision = \frac{TP}{TP + FP} \tag{3.6}$$

Recall indicates how many positive cases are classified as positive which is calculated as shown in equation 3.7;

$$Recall = \frac{TP}{TP + FN} \tag{3.7}$$

F1 Score is shown in equation 3.8;

$$F1\ Score = \frac{2\ x\ \text{Precision}\ x\ \text{Recall}}{\text{Precision} + \text{Recall}} \tag{3.8}$$

3.3 APPLIED PROCEDURES

It is quite difficult to obtain real-time images in the aviation field. Therefore, images from a previously prepared dataset are used in the study. Since this dataset contains thousands of images, images of different sizes were resized to a single size. In the first stage, since the input data size of the Resnet18 and GoogleNet models is 224x224x3, all images were converted to this format. Since all images in the dataset are RGB images, no action was taken for this situation. The resized images were randomly divided into image clusters with a ratio of 90% training and 10% test. These ratios are 75% training and 25% test, 50% training and 50% test, and 25% training and 75% test, respectively, and the clusters were created repeatedly for each new training. The model was trained with the images in the created training set. At the end of the training, testing was performed with the images in the test set created in the previous stage, and the result was obtained. All of these processes were repeated separately for image sizes 210x210x3, 230x230x3, and 250x250x3. The flow diagram describing a cycle of these processes is given in Figure 9.

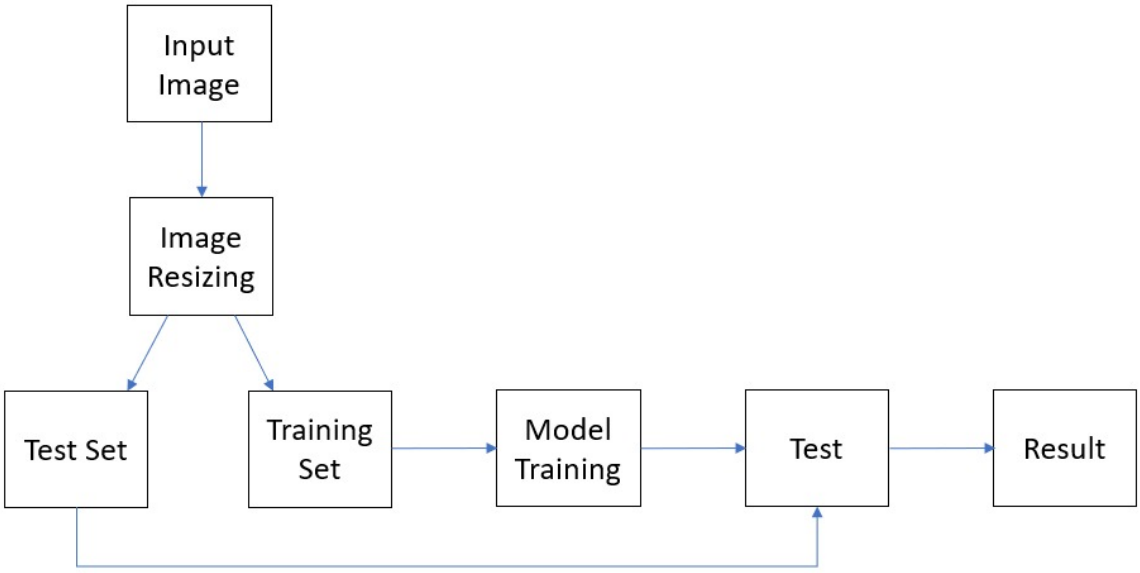

Figure 9: Flow Chart of the Methodology

CHAPTER IV
PRETRAINED NETWORKS USED IN STUDY

4.1 RESNET18

A neural network employed in computer vision tasks is ResNet18, which is a "Residual Network" with 18 layers. The ResNet model was developed to resolve the "vanishing gradient" issue that arises during the training of deep neural networks. This issue occurs when the gradients approach zero as the network deepens, which complicates the model's learning process.

ResNet's fundamental innovation is the implementation of "skip connections" or "residual connections." These connections enable the direct addition of the input of every few layers to the output. This guarantees that the model does not overlook the information from previous layers as it progresses to more complex layers.

- ResNet18 is extensively employed in a variety of computer vision tasks, including object detection, image classification, and segmentation. It is also appropriate for transfer learning, which entails the ability to fine-tune a pre-trained ResNet18 model for various tasks. In terms of both computational cost and efficacy, ResNet18 is a balanced model that is a preferred choice for a variety of applications [29]. ResNet-18 consists of 16 convolution layers, 2 subsampling layers and fully connected layers (fc). The input image size of ResNet is 224x224. In addition to the first convolution layer, the other layers are 3x3, and the convolution kernel size of ResNet is 7x7. After the average pooling of the feature map of the last convolution layer, an eigenvector is obtained with full connection, then the classification probability is obtained by normalization with Softmax. The calculation of the softmax is shown in equation 4.1.

$$\sigma(Z_i) = \frac{e^{z_i}}{\sum_{j=1}^{n} e^{z_j}} \tag{4.1}$$

where:

- z_i is the i-th component of the input vector z, n is the total number of components in the vector,
- e^{z_i} is the exponential of the i-th component.

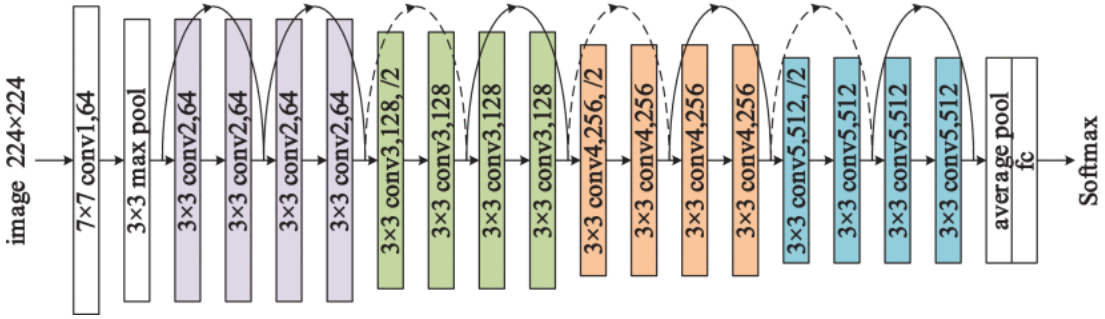

Figure 10: ResNet18 Architecture [30]

The 18 layers of ResNet18 are organized as shown in Figure 10. The initial layer is a 7x7 convolutional layer, which is succeeded by a 3x3 max pooling layer. Two convolutional layers and a residual connection are included in each block. These slabs are composed of 2, 2, 2, and 2 layers, respectively. Lastly, a completely connected layer is followed by a global average pooling layer.

4.2 GOOGLENET

The ILSVRC (ImageNet Large Scale Visual Recognition Challenge) competition was won by GoogleNet, a deep learning model that was developed by Google in 2014. It is also referred to as the Inception network. GoogleNet efficiently reduces computational costs while simultaneously achieving greater accuracy [31].

The architecture of GoogleNet is based on Inception modules, which enable the simultaneous extraction of features at different dimensions. These modules generate feature maps that are more detailed by concurrently applying filters of varying sizes. The architecture of GoogleNet is given in Figure 11.

GoogleNet is extensively employed in various computer vision tasks, including object detection, image classification, and segmentation. It is also appropriate for transfer learning, which enables the fine-tuning of a pre-trained GoogleNet model for various tasks.

GoogleNet is a model that is a preferable choice for a variety of applications due to its balanced computing cost and performance. The model's extensive and

comprehensive architecture allows it to capture a greater amount of information, as evidenced by its 22-layer deep structure. Inception modules maintain high accuracy while reducing computational cost.

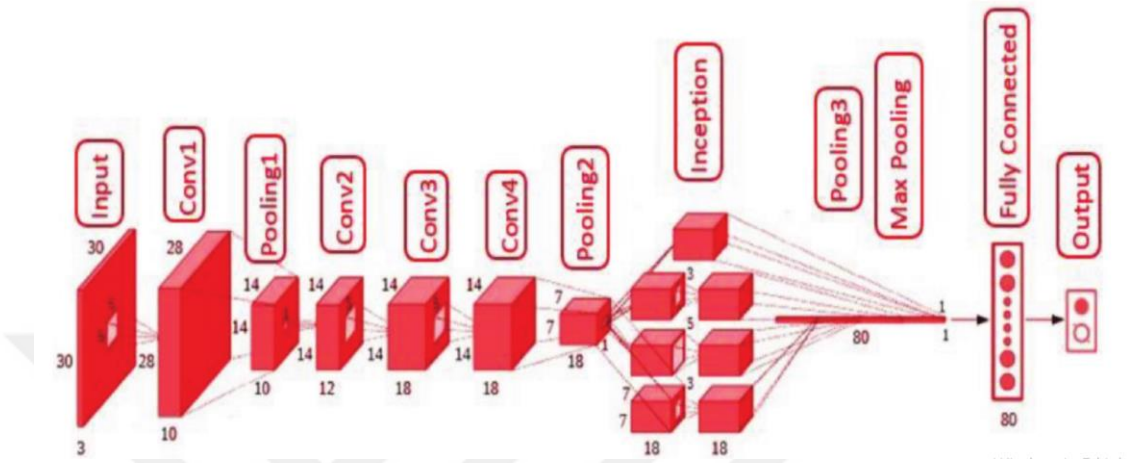

Figure 11: GoogleNet Architecture [32]

The initial layer is a 7x7 convolutional layer, which is succeeded by a 3x3 max pooling layer. The fundamental building blocks of GoogleNet, Inception modules, consist of convolutional layers with varying sizes (1x1, 3x3, 5x5) and a 3x3 max pooling layer. These modules facilitate the simultaneous extraction of features at various scales. A total of nine Inception modules are present throughout the network. Each module's output is passed through various convolutional and pooling layers. The final layer is a completely connected layer that is followed by a global average pooling layer. The softmax function is employed by the final layer to conduct classification [33].

CHAPTER V
EXPERIMENTAL RESULTS

The dataset used in the study contains 1429 Military Jet Aircraft, 1074 Helicopter, 868 Passenger Plane, 1223 Drone, 980 Missile.

The dataset is partitioned into training and testing sets by generating random groups with different proportions (10-90%, 25-75%, 50-50%, 75-25%) in order to enable a rigorous evaluation of the model.

Two state-of-the-art Convolutional Neural Network (CNN) models, ResNet-18 and GoogleNet, were selected for the classification tasks. The models were implemented using MATLAB, leveraging its deep learning toolbox.

The architecture of ResNet-18 consists of 18 layers, including convolutional, pooling, and fully connected layers. It employs residual connections to mitigate the vanishing gradient problem, allowing for deeper network training.

GoogleNet features a 22-layer deep structure with Inception modules, which allow for multi-scale feature extraction. This architecture reduces computational cost while maintaining high accuracy.

Performance metrics were calculated to see the results of the networks. The models' performance was assessed using multiple criteria, including accuracy, precision, recall, and F1 score. These measures offer a thorough comprehension of the models' classification abilities.

Table 2 shows the accuracy values for the Drone and Missile duo of the ResNet18 and GoogleNet models.

Table 2: Models Comparison for Drone and Missile

Drone-Missile						
Test Accuracies (%)		Test images (%)	75	50	25	10
		Training images (%)	25	50	75	90
	Pretrained Models	ResNet18	90,25	90,1	92,04	93,37
		GoogleNet	92,24	92,96	93,47	92,35

ResNet18 and GoogleNet results show that GoogleNet performance rate is more effective in three out of four different percentages. As can be seen from here, the performance increases as the number of data used for Resnet18 and GoogleNet training increases. Table 2 shows that for 75% training data, GoogleNet achieved 93.47% performance.

Table 3: Models Comparison for Drone and Passenger

Drone-Passenger						
Test Accuracies (%)		Test images (%)	75	50	25	10
		Training images (%)	25	50	75	90
	Pretrained Models	ResNet18	90,23	90,2	93,1	92,47
		GoogleNet	89,87	91,28	91,81	90,32

Table 3 shows that ResNet18 achieved the highest performance with 93.10% performance for 75% training data. It is clear from these two tables that the increase in training data has a positive effect on performance.

Table 4: Models Comparison for Helicopter and Drone

Helicopter-Drone						
Test Accuracies (%)		Test images (%)	75	50	25	10
		Training images (%)	25	50	75	90
	Pretrained Models	ResNet18	92,29	92,66	93,74	96,09
		GoogleNet	93,4	93,54	95,69	96,59

Table 5: Models Comparison for Helicopter and Missile

Helicopter-Missile						
Test Accuracies (%)		Test images (%)	75	50	25	10
		Training images (%)	25	50	75	90
	Pretrained Models	ResNet18	94,92	96,2	97,67	98,41
		GoogleNet	97,11	97,77	97,46	95,77

Table 6: Models Comparison for Helicopter and Passenger

Helicopter-Passenger						
Test Accuracies (%)		Test images (%)	75	50	25	10
		Training images (%)	25	50	75	90
	Pretrained Models	ResNet18	95,45	95,87	98,21	98,32
		GoogleNet	97,17	96,31	97,09	96,65

Table 7: Models Comparison for Jet and Helicopter

Jet-Helicopter						
Test Accuracies (%)		Test images (%)	75	50	25	10
		Training images (%)	25	50	75	90
	Pretrained Models	ResNet18	94,47	94,89	96,83	97,56
		GoogleNet	96,01	96,13	96,13	96,48

The table shows the results by matching 4,5,6,7 helicopter and other groups. As can be seen from these three tables, ResNet18 gives the highest performance for 90% of training data.

In Table 4, and Table 7 GoogleNet gives its highest performance for 90% of training data, while in Tables 5 and 6, this performance decreases slightly for 90% of training data. However, since the test and training data were taken randomly, such a small decrease in the performance rate can be ignored.

Table 8: Models Comparison for Jet and Drone

Jet-Drone						
Test Accuracies (%)		Test images (%)	75	50	25	10
		Training images (%)	25	50	75	90
	Pretrained Models	ResNet18	87	85,73	87,18	90,6
		GoogleNet	87,86	90	91,62	89,32

Table 9: Models Comparison for Jet and Passenger

Jet-Passenger						
Test Accuracies (%)		Test images (%)	75	50	25	10
		Training images (%)	25	50	75	90
	Pretrained Models	ResNet18	85,1	87,34	86,37	85,58
		GoogleNet	86,96	87,34	89,44	87,02

Table 10: Models Comparison for Jet and Missile

Jet-Missile						
Test Accuracies (%)		Test images (%)	75	50	25	10
		Training images (%)	25	50	75	90
	Pretrained Models	ResNet18	92,14	91,5	91,77	90,83
		GoogleNet	91,83	93,42	93,42	94,95

Table 11: Models Comparison for Passenger and Missile

Passenger-Missile						
Test Accuracies (%)		Test images (%)	75	50	25	10
		Training images (%)	25	50	75	90
	Pretrained Models	ResNet18	91,09	93,2	93,9	91,18
		GoogleNet	94,21	94,49	93,66	93,53

The Table 8, Table 9, Table 10 and Table 11 shows that the performance rates for the four different cases do not vary greatly. However, when the tables are evaluated in general, a large increase in the number of training data contributes positively to

performance. The fact that test and training data are randomly separated affects performance.

Table 12: Models Comparison for Drone, Helicopter and Missile

Drone-Helicopter-Missile						
Test Accuracies (%)		Test images (%)	75	50	25	10
		Training images (%)	25	50	75	90
	Pretrained Models	ResNet18	92,12	93,04	93,76	94,12
		GoogleNet	94,09	94,71	95,21	94,35

Table 13: Models Comparison for Drone, Helicopter and Passenger

Drone-Helicopter-Passenger						
Test Accuracies (%)		Test images (%)	75	50	25	10
		Training images (%)	25	50	75	90
	Pretrained Models	ResNet18	90,84	92,04	92,97	95,09
		GoogleNet	92,09	93,68	94	94,15

Table 14: Models Comparison for Drone, Jet and Helicopter

Drone-Jet-Helicopter						
Test Accuracies (%)		Test images (%)	75	50	25	10
		Training images (%)	25	50	75	90
	Pretrained Models	ResNet18	90,13	90,35	89,74	92,44
		GoogleNet	90,62	91,87	91,99	91,99

Table 15: Models Comparison for Drone, Jet and Missile

Drone-Jet-Missile						
Test Accuracies (%)		Test images (%)	75	50	25	10
		Training images (%)	25	50	75	90
	Pretrained Models	ResNet18	87,55	90,09	89,81	88,68
		GoogleNet	90,9	90,34	90,58	91,98

Table 16: Models Comparison for Drone, Jet and Passenger

Drone-Jet-Passenger						
Test Accuracies (%)		Test images (%)	75	50	25	10
		Training images (%)	25	50	75	90
	Pretrained Models	ResNet18	84,43	86,55	86,58	87,47
		GoogleNet	87,01	87,61	88,87	88,11

Table 17: Models Comparison for Drone, Missile and Passenger

Drone-Missile-Passenger						
Test Accuracies (%)		Test images (%)	75	50	25	10
		Training images (%)	25	50	75	90
	Pretrained Models	ResNet18	90,4	92,61	93,04	92,27
		GoogleNet	90,92	92,52	93,53	90,58

Table 18: Models Comparison for Helicopter, Missile and Passenger

Helicopter-Missile-Passenger						
Test Accuracies (%)		Test images (%)	75	50	25	10
		Training images (%)	25	50	75	90
	Pretrained Models	ResNet18	94,39	94,7	95,44	94,3
		GoogleNet	95,05	96,19	95,44	97,52

Table 19: Models Comparison for Jet, Helicopter and Missile

Jet-Helicopter-Missile						
Test Accuracies (%)		Test images (%)	75	50	25	10
		Training images (%)	25	50	75	90
	Pretrained Models	ResNet18	92,89	94,5	94,12	95,79
		GoogleNet	94,74	94,54	94,88	95,79

Table 20: Models Comparison for Jet, Helicopter and Passenger

Jet-Helicopter-Passenger						
Test Accuracies (%)		Test images (%)	75	50	25	10
		Training images (%)	25	50	75	90
	Pretrained Models	ResNet18	91,15	91,72	92,27	93,7
		GoogleNet	92,04	92,84	93,14	93,49

Table 21: Models Comparison for Jet, Missile and Passenger

Jet-Missile-Passenger						
Test Accuracies (%)		Test images (%)	75	50	25	10
		Training images (%)	25	50	75	90
	Pretrained Models	ResNet18	88,05	89,83	89,74	88,59
		GoogleNet	89,92	90,5	91,25	92,17

Table 12, Table 13, Table 14, Table 15, Table 16, Table 17, Table 18, Table 19 Table 20 and Table 21show the test results of five different data divided into groups of three. The increase in the number of judicial training data derived from all tables' results contributes positively to my performance. However, among the data presented in groups of three, it is seen that the presence of a helicopter has a positive impact on performance.

Table 22: Models Comparison for Drone, Helicopter, Missile and Passenger

Drone-Helicopter-Missile-Passenger						
Test Accuracies (%)		Test images (%)	75	50	25	10
		Training images (%)	25	50	75	90
	Pretrained Models	ResNet18	92,35	93,74	93,45	92,7
		GoogleNet	93,36	94,05	94,8	95,1

Table 23: Models Comparison for Drone, Jet Helicopter and Missile

Drone-Jet-Helicopter-Missile						
Test Accuracies (%)		Test images (%)	75	50	25	10
		Training images (%)	25	50	75	90
	Pretrained Models	ResNet18	91,53	92,1	92,11	92,49
		GoogleNet	92,15	92,69	92,76	93,52

Table 24: Models Comparison for Drone, Jet, Helicopter and Passenger

Drone-Jet-Helicopter-Passenger						
Test Accuracies (%)		Test images (%)	75	50	25	10
		Training images (%)	25	50	75	90
	Pretrained Models	ResNet18	91,16	90,9	92,35	90,79
		GoogleNet	90,77	91,75	92,19	94,67

Table 25: Models Comparison for Drone, Jet, Missile and Passenger

Drone-Jet-Missile-Passenger						
Test Accuracies (%)		Test images (%)	75	50	25	10
		Training images (%)	25	50	75	90
	Pretrained Models	ResNet18	88,73	89,94	89,83	91,07
		GoogleNet	89,91	90,69	91,42	91,2

Table 26: Models Comparison for Jet, Helicopter, Missile and Passenger

Jet-Helicopter-Missile-Passenger						
Test Accuracies (%)		Test images (%)	75	50	25	10
		Training images (%)	25	50	75	90
	Pretrained Models	ResNet18	91,59	92,34	93,19	92,78
		GoogleNet	92,73	93,87	93,02	93,99

The Table shows the test results of four groups of five different data 22,23,24,25 and 26. As can be seen from these tables, the increase in the number of training data contributes positively to performance. Again, it can be seen here that the

fact that helicopter data is included in the training and test data also contributes positively to the test success rate.

Table 27: Models Comparison for Jet, Passenger, Drone, Missile and Helicopter

Jet-Passenger-Drone-Missile-Helicopter						
Test Accuracies (%)		Test images (%)	75	50	25	10
		Training images (%)	25	50	75	90
	Pretrained Models	ResNet18	90,91	91,72	92,69	91,97
		GoogleNet	92,28	93,11	93,1	95,23

Table 27 shows the test performance rates when all five different data are used in training and testing. GoogleNet gives much higher performance than ResNet18 when the number of training data is maximum. Accordingly, the more training data there is, the higher the test success rate can be.

As a result of all these results, situations with a high number of training data generally lead to the highest performance. Since these five classes will be used as test data, these five classes should also be included in the training data. For this reason, in order to find the average performance for cases where five classes participated in the training and test groups and the training data was maximum, the training were repeated five times, and the average performance metrics are presented for ResNet18 in Table 28 and for GoogleNet in Table 28. In addition, the dimensions of the input image were changed to observe ResNet18 and GoogleNet performances. While the input image dimensions of ResNet18 and GoogleNet were 224x224x3, the input layer was intervened and the input dimensions were retrained as 210x210x3, 230x230x3, 250x250x3. In this way, the effect of the size of the input image on the performance was observed.

Table 28: Different Input Size Comparison of ResNet18 and Performance Metrics

Jet-Passenger-Drone-Missile-Helicopter								
Test Accuracies (%)	Training Images (%90) - Test images (%10)							
	Pretrained Models	Metrics	1st Test	2nd Test	3rd Test	4th Test	5th Test	Avg Test
	ResNet18	Test Accuracy	93,53	94,12	94,67	92,6	93,89	93,762
		Recall	83,57	84,97	86,94	81,68	84,93	84,418
		Precision	84,42	85,53	86,74	81,67	85,28	84,728
		F1_Score	83,76	85,22	86,82	81,67	85,03	84,5
	ResNet18 (210 210)	Test Accuracy	93	94,43	93,72	93,72	93,96	93,766
		Recall	82,6	85,99	84,56	84,4	85,06	84,522
		Precision	82,82	86,63	84,75	84,48	85,48	84,832
		F1_Score	82,69	86,27	84,65	84,42	85,19	84,644
	ResNet18 (230 230)	Test Accuracy	94,27	94,35	95,31	94,67	93,32	**94,384**
		Recall	85,95	86,1	88,39	86,6	83,71	86,15
		Precision	86,14	85,96	88,53	87,06	83,85	86,308
		F1_Score	86	85,99	88,4	86,79	83,76	86,188
	ResNet18 (250 250)	Test Accuracy	93,08	93,24	93,08	93,16	92,68	93,048
		Recall	82,79	83,62	83,18	82,88	81,61	82,816
		Precision	83,58	83,37	83,23	83,11	82,27	83,112
		F1_Score	83,1	83,46	83,1	82,98	81,89	82,906

Table 28 shows all the performance metrics of ResNet18 when the input image sizes are different for the 10% of tests and 90% of training cases. Performance metrics reached the maximum when the input image was 230x230x3. The accuracy and loss graph of this training is given in Figure 13. As the size of the input image increases, performance increases. However, the performance decreases when the 224x224x3 input image is enlarged to 250x250x3. This means that when the size of the image is enlarged by resizing, the image begins to deteriorate. This has a negative impact on education. However, it can be seen that some growth contributes to the test result. The accuracy graph of all ResNet18 models with changed input dimensions is given in Figure 12.

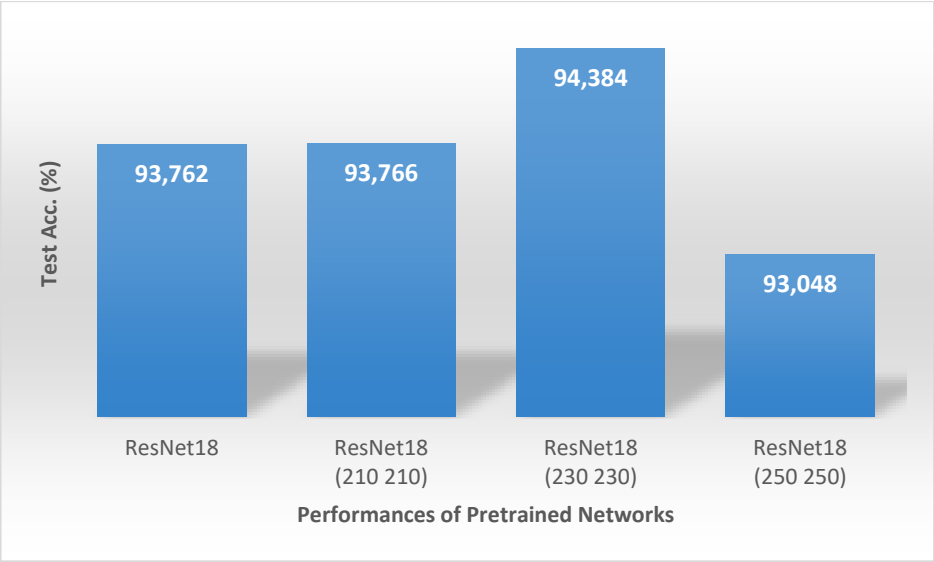

Figure 12: Performance Comparison of Different Input Size of ResNet18

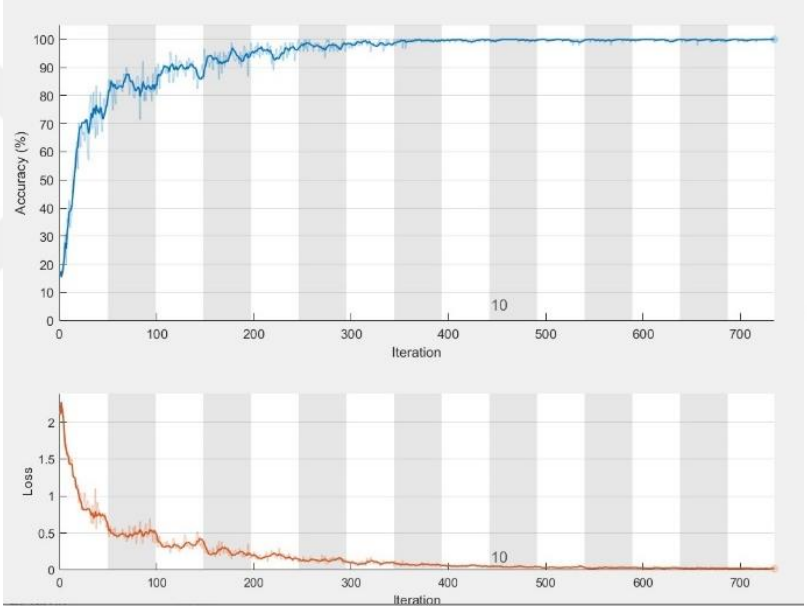

Figure 13: ResNet18 230x230x3 Accuracy & Loss Graph

Table 29: Different Input Size Comparison of GoogleNet and Performance Metrics

Jet-Passenger-Drone-Missile-Helicopter								
Test Accuracies (%)	Training Images (%90) - Test images (%10)							
	Pretrained Models	Metrics	1st Test	2nd Test	3rd Test	4th Test	5th Test	Avg Test
	GoogleNet	Test Accuracy	94,91	93,88	94,12	94,27	94,35	94,306
		Recall	87,33	84,49	85,5	85,63	86,68	85,926
		Precision	87,8	85,32	86,54	85,89	86,28	86,366
		F1_Score	87,42	84,81	85,89	85,69	86,15	85,992
	GoogleNet (210 210)	Test Accuracy	94,27	94,83	94,35	94,91	94,12	**94,496**
		Recall	86,19	87,02	86	87,19	85,44	86,368
		Precision	86,15	87,54	86,31	87,8	85,44	86,648
		F1_Score	86,1	87,14	86,08	87,35	85,42	86,418
	GoogleNet (230 230)	Test Accuracy	94,99	94,19	94,35	94,27	92,6	94,08
		Recall	87,35	85,05	85,2	85,56	81,75	84,982
		Precision	87,83	85,99	87,92	86,5	82,19	86,086
		F1_Score	87,48	85,45	86,18	85,93	81,92	85,392
	GoogleNet (250 250)	Test Accuracy	94,51	94,67	93,32	94,41	92,6	93,902
		Recall	86,48	86,54	83,37	85,95	81,75	84,818
		Precision	86,49	86,86	83,91	86,79	82,19	85,248
		F1_Score	86,47	86,58	83,57	86,31	81,92	84,97

Table 29 shows all the performance metrics of GoogleNet in cases where the input image sizes are different, for 10% of tests and 90% of training cases, as in ResNet18. In GoogleNet, performance metrics reached the maximum when the input image was 210x210x3, unlike ResNet. The accuracy and loss graph of this training is given in Figure 15. While the performance in ResNet is negatively affected as the size of the input image increases, GoogleNet is not significantly affected by this situation. However, it is seen that GoogleNet performance is highest when the input image from 224x224x3 is reduced to 210x210x3. Reducing the size of the input image reduces the processor load compared to other cases. While this reduction is a gain, the fact that performance is also increasing is a great advantage for the system. When all these results are compared, GoogleNet shows a better performance when the training data is maximum and the data size is small.

These two tables show that the difference between the average test performance rate of the five-time training when the input size of the ResNet18 image, which gives the best results, is 230x230x3 and the input size of the GoogleNet image is 210x210x3, is 0.138. In the case of ResNet18 230x230x3, the average training time is 21 minutes, while in the case of GoogleNet 210x210x3, the average training time is 51.5 minutes.

The test performance difference of 0.138 shows that ResNet18 offers more than half the time saving compared to GoogleNet in cases where it is not vital for the system. The accuracy graph of all GoogleNet models with changed input dimensions is given in Figure 14.

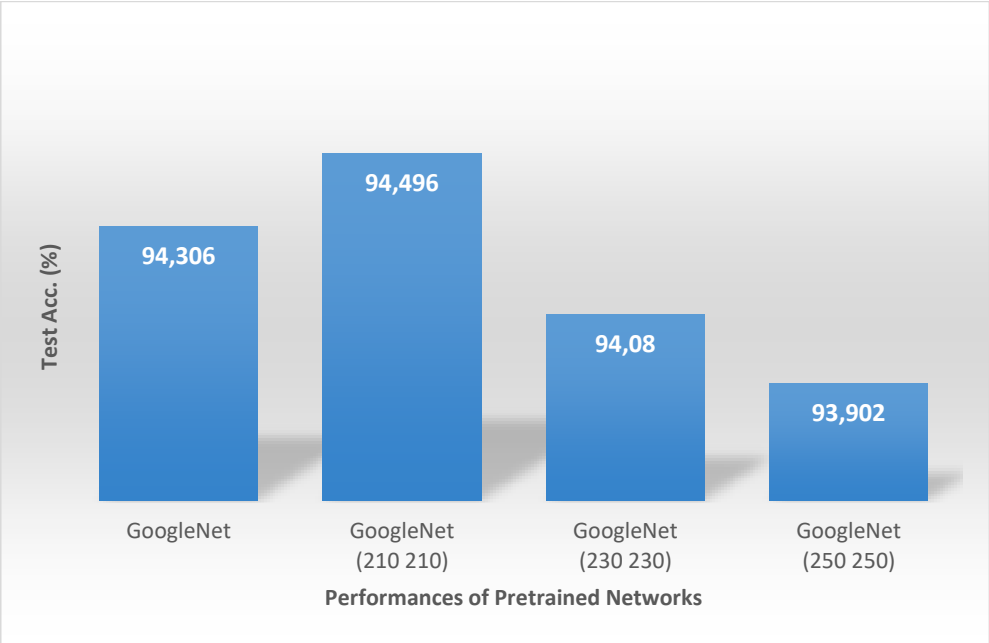

Figure 14: Performance Comparison of Different Input Size of GoogleNet

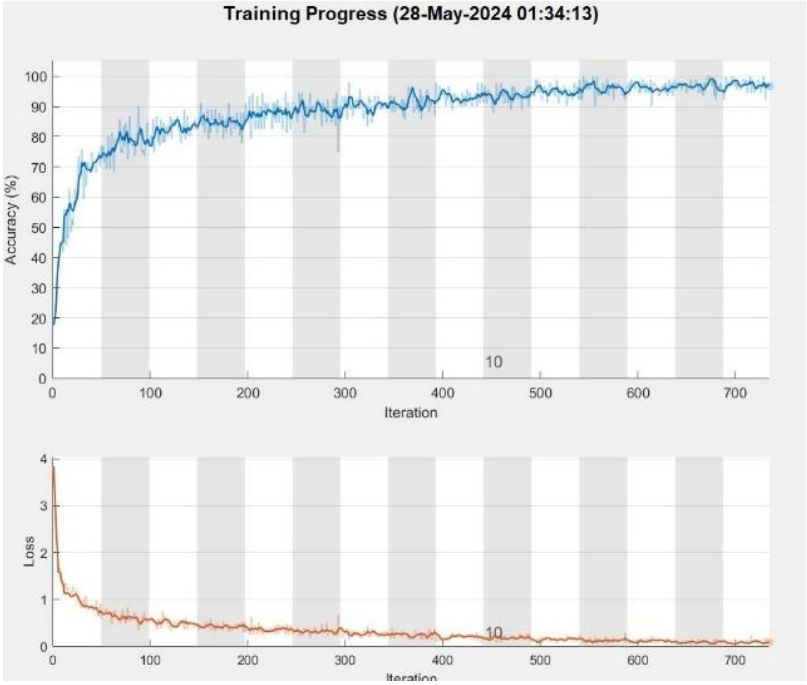

Figure 15: GoogleNet 210x210x3 Accuracy & Loss Graph

CHAPTER VI
CONCLUSION AND DISCUSSION

The main purpose of this study is to reach more precise conclusions in the classification of aircraft on issues such as airspace security and aircraft detection.

A ready dataset was used in this study. This dataset includes 5 different aircraft classes: military jet aircraft, passenger aircraft, helicopters, drones and missiles.

Image classification technique is used in medical imaging, automotive industry, security systems, agriculture, unmanned systems and many other fields. Image classification was used in this study to classify aircraft consisting of 5 separate data. While using this, performance analysis on the dataset was performed with different CNN models such as ResNet18 and GoogleNet. For this performance analysis, different percentages of training and testing datasets were randomly generated: 10%, 25%, 50%, and 75%. While the input data size of both ResNet18 and GoogleNet models was 224x224x3, all classes were trained separately in twos, threes, fours and fives and the performances among themselves were analyzed. It was observed that my performance directly reached high levels in the trainings where the helicopter class was included. In other trainings, it was observed that the performance rate of trainings with more data was generally higher than trainings with less data. Based on these results, both models were trained five times with randomly generated clusters and 90% data, and the average performance rate was calculated. At the same time, training was carried out separately by increasing and decreasing the input data size of both models. As a result of these trainings, the best performance rate was obtained when the input data size of the GoogleNet model was 210x210x3 and the performance rate was 94.496%. In the ResNet18 model, the highest performance rate of 94.384% was achieved and the input data size is 230x230x3. In this study, the effect of changes in the input data size on image classification was observed.

This study presents the performance analysis of ResNet18 and Googlenet for images on the dataset given in [15]. In this study, better results were obtained by changing the input data sizes of ResNet18 and GoogleNet models compared to their

original sizes. Although GoogleNet gave better results between the 230x230x3 dimensional ResNet18 modeland the 210x210x3 dimensional GoogleNet model, the difference between them is 0.112%. Training times are on average 21 minutes for ResNet18 and 51.5 minutes for GoogleNet. It has been concluded that using the GoogleNet model with 210x210x3 inputs if the performance difference is at critical levels, and using the ResNet18 model with 230x230x3 inputs if the time difference is critical, gives the best performance in the classification of aircraft.

As the training data increased, better and more stable results were observed. The limited data sets limit the studies. The diversity of datasets and increased content numbers will pave the way for this and similar studies and will create the opportunity to obtain more accurate and stable results. While the target is high performance, there is a high dataset requirement, which is among the limitations of the study. It is thought that the study can achieve higher performance when these constraints are resolved.

REFERENCES

[1] PANDA B. S., GOPAL K. M., SATPATHY R. and PANDA G. (2024), "Detection and Recognition of Aircraft Vehicle-A Supple Approach Using Deep Pliable Yolov5", *Multimedia Tools and Applications*, pp. 1-22, DOI: 10.1007/s11042-024-19597-8.

[2] SHEN M., YANG F., WEN P., SONG B. and LI, Y. (2024), "A Real-Time Epilepsy Seizure Detection Approach Based on EEG Using Short-Time Fourier Transform and Google-Net Convolutional Neural Network", *Heliyon*, Vol. 10, No. 11e31827.

[3] GUO M. and DU Y. (2019), "Classification of Thyroid Ultrasound Standard Plane Images Using Resnet-18 Networks", *2019 IEEE 13th International Conference on Anti-Counterfeiting, Security, and Identification (ASID)*, pp. 324-328, IEEE, DOI: 10.1109/ICASID.2019.8925267.

[4] SPANHOL F. A., OLIVEIRA L. S., PETITJEAN C. and HEUTTE L. (2015), "A Dataset for Breast Cancer Histopathological Image Classification", *IEEE Transactions on Biomedical Engineering*, Vol. 63, No. 7, pp. 1455-1462, DOI: 10.1109/TBME.2015.2496264.

[5] SHIFAT E., RABBI M., YIN X., FITZGERALD C. E. and ROHDE G. K. (2020), *"*Cell Image Classification: A Comparative Overview*", Cytometry Part A*, Vol. *97*, No. 4, pp. 347-362, DOI: 10.1002/cyto.a.23984.

[6] ZHUANG Q., GAN S. and ZHANG L. (2022), "Human-Computer Interaction Based Health Diagnostics Using Resnet34 for Tongue Image Classification", *Computer Methods and Programs in Biomedicine*, Vol. 226, Article 107096, DOI: 10.1016/j.cmpb.2022.107096.

[7] HSIEH T. H. and KIANG J. F. (2020), "Comparison of CNN Algorithms on Hyperspectral Image Classification in Agricultural Lands", *Sensors*, Vol. 20, No. 6, p. 1734, DOI: 10.3390/s2006173.

[8] HASHEMI-BENI L. and GEBREHIWOT A. (2020), “Deep Learning for Remote Sensing Image Classification for Agriculture Applications”, *The International Archives of Photogrammetry, Remote Sensing and Spatial Information Sciences*, Vol. XLIV-M-2-2020, pp. 51-54, DOI: 10.5194/isprs-archives-XLIV-M-2-2020-51-2020.

[9] KHUMALO M., MUDUVA M., TARAMBIWA E., MUSANGA V. and CHIWARIRO R. (2023), “Aircraft identification using machine learning”, *IJIRT*, Vol. 9, No. 8, pp. 713-724.

[10] LIU H., QU F., LIU Y., ZHAO W. and CHEN Y. (2018), “A Drone Detection with Aircraft Classification Based on A Camera Array”, *IOP Conference Series: Materials Science and Engineering*, Vol. 322, No 5, p. 052005, DOI: 10.1088/1757-899X/322/5/052005.

[11] CHEN J., LI H. and ZHANG G. (2020), “Dataset of Aircraft Classification in Remote Sensing Images”, *Journal of Global Change Data & Discovery*, Vol. 4, No. 2, pp. 183-190, DOI: 10.3974/geodp.2020.02.12.

[12] BOLTON S., DILL R., GRIMAILA M. R. and HODSON D. D. (2023), “Multi-Sensor Aircraft Classification”, *2023 Congress in Computer Science, Computer Engineering, & Applied Computing (CSCE)* pp. 796-800, IEEE, DOI: 10.1109/CSCE60160.2023.00136.

[13] WANG Y., CHEN Y. and LIU R. (2022), “Aircraft Image Recognition Network Based on Hybrid Attention Mechanism”, *Computational Intelligence and Neuroscience*, Vol. 2022, No. 1, p. 4189500, DOI: 10.1155/2022/4189500.

[14] CHEN X., WANG X., SPITZLEY L. and NUNAMAKER J. (2023), “Trust and deception with high stakes: Evidence from the friend or foe dataset”, *Decision Support Systems*, Vol. 173, p113997, DOI: 10.1016/j.dss.2023.113997.

[15] WAHEED Abdul (2019), *Flying-Planes*, https://www.kaggle.com/datasets/eabdul/flying-vehicles, DoA. 08.02.2024.

[16] FEDERAL AVIATION ADMINISTRATION (2023), *Aircraft Characteristics Database*, https://www.faa.gov/airports/engineering/aircraft_char_database/data, DoA. 15.05.2024.

[17] ROBERT G. L. (2023), *Encyclopedia of Physical Science and Technology*, 3th Edition, Robert A. Meyers, Academic Press, San Diego.

[18] HELICOPTER FLIGHTS (2024), *Helicopter Technology*, https://www.helicopterflights.com/en/docs/show/22/helicopter-technology, DoA. 25.08.2024.

[19] SHAH P. Z. (2009), "*Pakistan Says us Drone Kills 13"*, 18 June 2009, https://www.nytimes.com/2009/06/19/world/asia/19pstan.html, DoA. 17.07.2024.

[20] SHARMA A., VANJANI P., PALIWAL N., BASNAYAKA C. M. W., JAYAKODY D. N. K., WANG H. C. and MUTHUCHIDAMBARANATHAN P. (2020), "Communication and Networking Technologies for Uavs: A Survey", *Journal of Network and Computer Applications,* Vol. 168, p. 102739, DOI: 10.1016/j.jnca.2020.102739.

[21] LINDSAY G. W. (2021), "Convolutional Neural Networks as a Model of The Visual System: Past, Present, and Future", *Journal of Cognitive Neuroscience*, Vol. 33, No. 10, pp. 2017-2031, DOI: 10.1162/jocn_a_01544.

[22] BALAJI S. (2020), *Binary Image Classifier CNN Using TensorFlow*, https://medium.com/techiepedia/binary-image-classifier-cnn-using-tensorflow, DoA. 11.07.2024.

[23] GHADERIZADEH S., ABBASI-MOGHADAM D., SHARIFI A., ZHAO N. and TARIQ A. (2021), "Hyperspectral Image Classification Using a Hybrid 3D-2D Convolutional Neural Networks", *IEEE Journal of Selected Topics in Applied Earth Observations and Remote Sensing*, Vol. 14, pp. 7570-7588, DOI: 10.1109/JSTARS.2021.3099118.

[24] YASIN M., SARIGÜL M. and AVCI M. (2024), "Logarithmic Learning Differential Convolutional Neural Network", *Neural Networks*, Vol. 172, p. 106114, DOI: 10.1016/j.neunet.2024.106114.

[25] BARBER F. B. N. and OUESLATI A. E. (2024), "Human Exons and Introns Classification Using Pre-Trained Resnet-50 and Googlenet Models and 13-Layers CNN Model", *Journal of Genetic Engineering and Biotechnology*, Vol. 22, No. 1, pp. 100359, DOI: 10.1016/j.jgeb.2024.100359.

[26] AKGÜL I. (2024), "A Pooling Method Developed for Use in Convolutional Neural Networks", *CMES-Computer Modeling in Engineering & Sciences*, Vol. 141, No. 1, pp. 751-770, DOI: 10.32604/cmes.2024.052549.

[27] MEDIUM (2024), *Deep Learning from Deepest*, https://medium.com/deep-learning-from-deepest, DoA. 14.07.2024.

[28] WANG J., XIA L. and LI S. (2021), "Research on Aircraft Type Recognition from Remote Sensing Images in Complex Scenes", *2021 International Conference on Computer Information Science and Artificial Intelligence (CISAI)*, pp. 995-1000, IEEE, DOI: 10.1109/CISAI54367.2021.00199.

[29] DAI S., XUE Y., ZHU Z. and QIN H. (2023), "Fault Diagnosis of Underwater Robot Propulsion Based on ResNet18 Network", *2023 5th International Conference on Frontiers Technology of Information and Computer (ICFTIC)*, pp. 1121-1125, IEEE, DOI: 10.1109/ICFTIC59930.2023.10456361.

[30] OU X., YAN P., ZHANG Y., TU B., ZHANG G., WU J. and LI W. (2019), "Moving Object Detection Method Via Resnet-18 with Encoder–Decoder Structure in Complex Scenes", *IEEE Access*, Vol. 7, pp. 108152-108160, DOI: 10.1109/ACCESS.2019.2931922.

[31] RUSSAKOVSKY O., DENG J., SU H., KRAUSE J., SATHEESH S., MA S. and FEI-FEI L. (2015), "Imagenet Large Scale Visual Recognition Challenge", *International Journal of Computer Vision*, Vol. 115, pp. 211-252, DOI: 10.1007/s11263-015-0816-y.

[32] ALKAN A., ABDULLAH M. U., ABDULLAH H. O., ASSAF M. and ZHOU H. (2021), "A Smart Agricultural Application: Automated Detection of Diseases in Vine Leaves Usinghybrid Deep Learning", *Turkish Journal of Agriculture and Forestry*, Vol. 45, No. 6, pp. 717-729, DOI: 10.3906/tar-2007-105.

[33] SHI B., ZHANG X., WANG Z., SONG J., HAN J., ZHANG Z. and TOE T. T. (2022), "GoogLeNet-Based Diabetic-Retinopathy-Detection", *2022 14th International Conference on Advanced Computational Intelligence (ICACI)*, pp. 246-249), IEEE, DOI: 10.1109/ICACI55529.2022.9837677.